TÜBİTAK

Turkish Journal of Chemistry

http://journals.tubitak.gov.tr/chem/

Research Article

Turk J Chem
(2019) 43: 730 – 739
© TÜBİTAK
doi:10.3906/kim-1808-12

Effect of crosslinking patterns on the properties of conjugated microporous polymers

Hakan BİLDİRİR*
Marmara Research Center, Scientific and Technological Research Council of Turkey (TÜBİTAK), Kocaeli, Turkey

Received: 03.08.2018 • **Accepted/Published Online:** 11.02.2019 • **Final Version:** 03.04.2019

Abstract: Syntheses and detailed spectroscopic characterizations of two similar conjugated microporous polymers formed by A4 + B2 and A2 + B3 type functional monomers via Sonogashira–Hagihara polycondensation are presented in this report. The two porous polymeric networks possess mono-, di-, and tri- (1-, 1,4-, and 1,3,5-, respectively) substituted benzene rings and fused thiophenic moieties (dithienothiophenes). Because of the different conjugation patterns, their solid state nuclear magnetic resonance, infrared, and ultraviolet/visible light absorption analyses indicated significant differences. Besides the discussions on the porous properties of the obtained polymeric networks, the presented spectroscopic investigations can be useful for identifying the structure-property relationship of the novel conjugated porous polymeric structures, since the characterization of such nonsoluble compounds by using fundamental techniques is always a challenge.

Key words: Porous organic polymers, conjugated microporous polymers, porous materials, dithienothiophenes, structure-property relationship, solid-state materials

1. Introduction

The porous organic polymers (POPs) are porous materials composed solely of organic building blocks.[1] As an advantage of their thermally and chemically stable backbone, which exhibits large accessible surface areas, POPs demonstrate competitive performances in traditional applications such as gas storage and heterogeneous catalysis,[2,3] although these areas are still dominated by their inorganic (i.e. zeolites) and organic-inorganic hybrid counterparts (i.e. metal-organic frameworks), respectively.[4–8] High electron density of POPs makes them promising materials for optoelectronic applications.[9–11] Conjugated POPs, namely conjugated microporous polymers (CMPs), are especially favorable materials for nanoelectronic systems due to their electron-rich and porous 3D skeletons, providing advanced electronic properties when compared to their conventional linear analogues.[12,13]

The key factor that separates POPs from the conventional polymers is that at least one of their building blocks should maintain more than two functional and polymerizable groups pointing in two or three dimensions, and all the monomers should be rigid to prevent the collapse of the porous skeleton.[14] It should be noted that there are also examples of POPs built from relatively flexible building blocks such as hypercrosslinked polymers,[15–18] the porous properties of which might vary depending on the conditions (i.e. humidity and pressure).[19,20]

*Correspondence: hakanbildirir@gmail.com

POPs can be obtained by using the numerous strategies that have been applied for traditional polymer syntheses for decades, and the selected technique will have a great impact on the final properties of the material.[13,21] For example, monomers functionalized with several specific groups to form boronic acid esters, imines, or similar groups (i.e. boroxine, hyrazone) can reversibly connect/disconnect to form the most thermodynamically stable compound (the process is called dynamic covalent chemistry) under solvothermal conditions, yielding crystalline POPs (covalent organic frameworks).[22−24] On the other hand, the standard put-and-stir wet polymer chemistry results in amorphous structures due to the irreversible connections, which generally concerns C-C bonded materials.[13] Thus, the carbon-carbon coupling methods are frequently used in the syntheses of amorphous POPs, the physical and electronic properties of which are affected by the reaction conditions.[21] For example, Yamamoto coupling is one of the earliest and most efficient methods in POP syntheses, which takes place between halogen functionalized monomers.[25,26] This coupling reaction is popular as it yields high surface area POPs; however, only homopolymers or random copolymers can be produced by using this method.[27,28] Suzuki-Miyaura cross-coupling is another frequently used strategy to produce alternating polymers.[21] The reaction takes place between halogen and boronic acid (or boronic acid ester) under basic conditions.[29] In that context, one should consider that such basic conditions may not be suitable for some compounds. In particular, if an aqueous base is used in the reaction, the presence of water may lead to poor solubility, resulting in an early precipitation of such highly rigid systems. Another alternating polymerization technique, which takes place between acetylene and halogen bearing compounds, Sonogashira–Hagihara polycondensation, is also effective in producing alternating POPs under mild reaction conditions.[21] This carbon-carbon coupling reaction became highly popular after the pioneering CMP study by Cooper et al.[30] and still is one of the most frequently used methods to form electron-rich POPs.

Due to their extended crosslinking and rigidity, POPs are nonsoluble materials in general and hence the investigations to identify their structure-property relationship can be a significant challenge.[21] Given that, there are numerous works representing successful spectral and physical characterizations of POPs obtained under controlled conditions via tuning the monomer ratio, time, solvent, temperature, catalyst, etc.[31−38] Similarly, in order to monitor their electronic properties, adjustment of the conjugation style and length by modifying the heteroatom-rich monomers has also been employed.[39−41] The choice of the monomers was also reported to have particularly significant effects on the electronic levels of CMPs.[42−45] For example, a CMP based on oxidation and reduction of a dithienothiophene (DTT, an aromatic heterocyclic system formed from three fused thiophenes)[46] via respective iodine and ammonia treatment was demonstrated in the literature.[47] On the other hand, another CMP built from a stronger electron-donating unit (tetrathiafulvalenes) could only be irreversibly doped by iodine exposure.[35]

In this work, the Sonogashira–Hagihara cross-coupling strategy was applied to produce CMPs from highly electron-rich di- and tetra-bromo DTT units and commonly used acetylene sources, namely tri- and di-ethynyl benzenes, respectively (Figure 1). As a result of the unidentical crosslinking, the nature of the formed voids was identified as not being the same. Hence, the gas sorption measurements revealed altered porous properties, as well as their spectral responses since the conjugation style was changed due to tri- and tetra- functionalized crosslinkers. Thus, the presented results are intended to help researchers to characterize such nonsoluble systems since the presented work involves a common method to produce POPs.

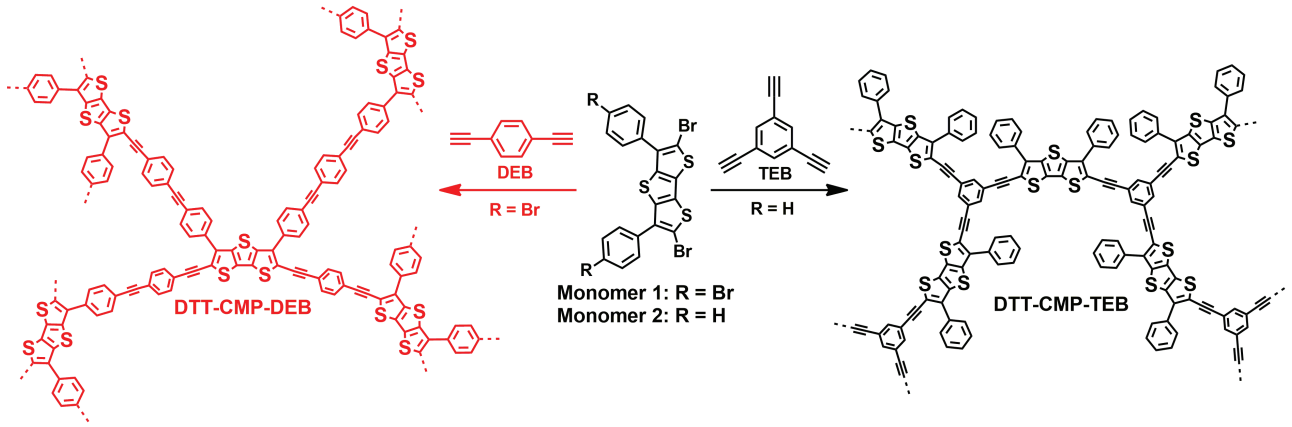

Figure 1. Reaction pathways for randomly A4 + B2 connected DTT-CMP-DEB and A2 + B3 type DTT-CMP-TEB formation.

2. Results and discussion

Sonogashira–Hagihara polycondensation was employed for A2 + B3 and A4 + B2 type functional monomers (A and B represent DTT and ethynylbenezenes, respectively) to produce the target POPs, namely DTT-CMP-TEB and DTT-CMP-DEB, in order to monitor the effects of different crosslinkings on their physical and electronic properties. Since the reaction was not solvothermal, the obtained powders were found to be amorphous after powder X-ray diffraction (p-XRD) analysis (Figure 2). Gas (N_2) sorption measurements of the polymers were performed to verify if the synthesized polymers possessed any accessible surface area. The gas sorption isotherm of DTT-CMP-DEB showed Type I behavior[24] with high N_2 uptake at low relative pressures, pointing to a better microporous character in comparison to DTT-CMP-TEB, which displayed a lower uptake in the studied region (Figure 3). DTT-CMP-DEB exhibited a much larger Brunauer–Emmett–Teller (BET) surface area of 513 $m^2\ g^{-1}$ compared to 197 $m^2\ g^{-1}$ for DTT-CMP-TEB. The larger surface area of the former was attributed to the higher number of micropores along its skeleton, which is probably due to the higher number of crosslinking sites (4 sites of DTT in the A4 + B2 type polycondensation), and also the shorter comonomer (DEB).[33] A higher fraction of micropore volume of DTT-CMP-DEB was also noted with respect to DTT-CMP-TEB (Table), as expected.[36] Furthermore, both isotherms showed a continuous further uptake of nitrogen in the intermediate pressure range, especially distinct for DTT-CMP-TEB. This continuous uptake as well as the large hysteresis of the desorption branch were attributed to a partial swelling of the polymers during gas uptake, which can be expected to be more pronounced for networks with lower crosslinking density.

Table. Reaction pathways for randomly A4 + B2 connected DTT-CMP-DEB and A2 + B3 type DTT-CMP-TEB formation.

	Surface area (BET – m^2g^{-1})	Pore size[a] (nm)	$V^b_{0.1}$ (cm^3g^{-1})	V^b_{tot} (cm^3g^{-1})	$V_{0.1}/V_{tot}$
DTT-CMP-TEB	197	2.1	0.069	0.27	0.26
DTT-CMP-DEB	513	1.4	0.20	0.30	0.67

[a]Dominant pore size, see inset of Figure 1. [b] $V_{0.1}$ and V_{tot} were calculated from the pore volume at $P/P_0 = 0.1$ and $P/P_0 = 0.9$, respectively.

^{13}C cross-polarization magic angle spinning (CP-MAS) solid state nuclear magnetic resonance (^{13}C-MAS-NMR) measurements were employed for both DTT-based CMPs. Resonances in aromatic and acetylenic

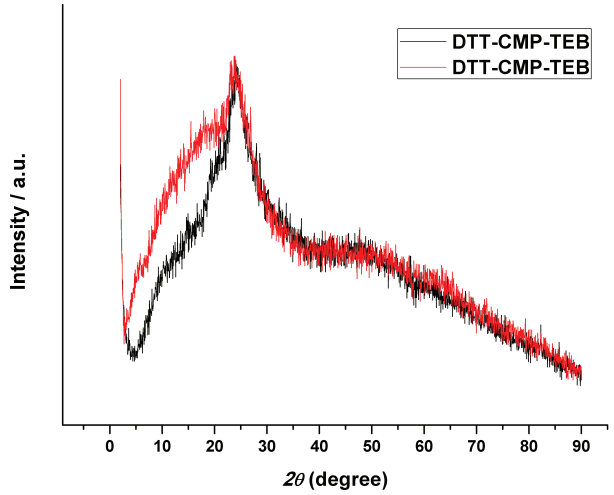

Figure 2. p-XRD measurements of DTT-CMP-DEB and DTT-CMP-TEB indicating the amorphous nature of the products.

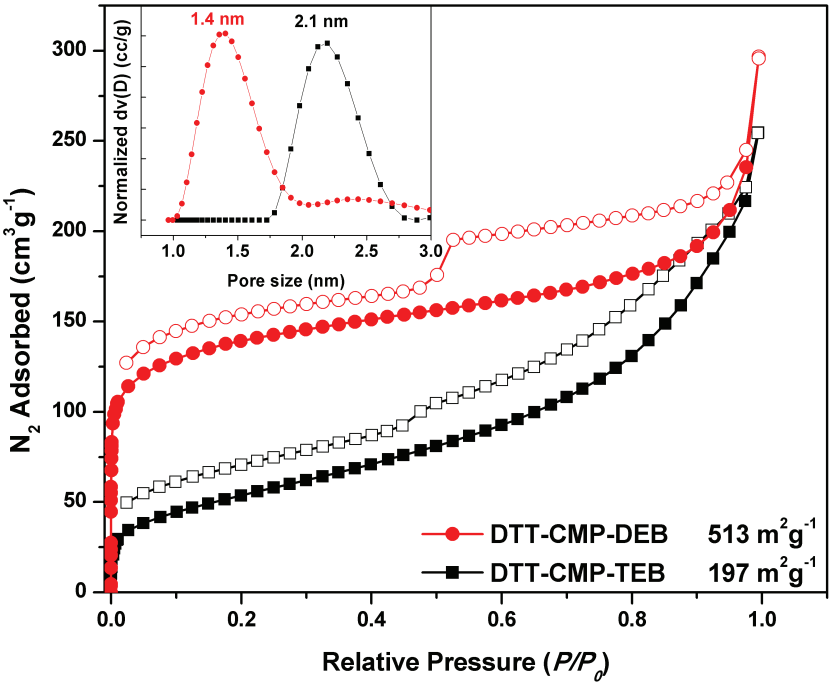

Figure 3. Gas sorption isotherms of DTT-CMP-DEB and DTT-CMP-TEB (QS DFT pore size distributions are shown on inset graph).

regions were clearly identified and assigned to the distinct moieties,[33,37,48] even though the observed peaks were relatively broad (Figure 4), which is not unexpected for solid state measurements of such amorphous materials. The most significant difference in the aromatic region was the higher intensity and sharpness of the 3°carbon peaks of the benzene moieties of DTT-CMP-DEB around 128 ppm with respect to the broad distribution of C-Hs in DTT-CMP-TEB in the aromatic region. The reason for the high intensity could be the larger population of 1,4-functionalized benzenes in DTT-CMP-DEB (from the linker DEB and the phenyl

substituents of DTT core). The characteristic aromatic carbon peaks of acetylene-bearing monomers around 129 ppm and 120 ppm (128.2 ppm and 120.4 ppm for DEB, 129.5 ppm and 121.0 ppm for TEB) and resonances of α-carbons of DTT moieties around 137 ppm (137.1 ppm for DTT-CMP-DEB, 135.6 ppm for DTT-CMP-TEB) can be observed in that region. Moreover, the peaks around 125 ppm could be assigned to β-carbons of DTTs; however, they were hindered, especially in the case of DTT-CMP-TEB due to the intense peaks of its phenyl side groups.

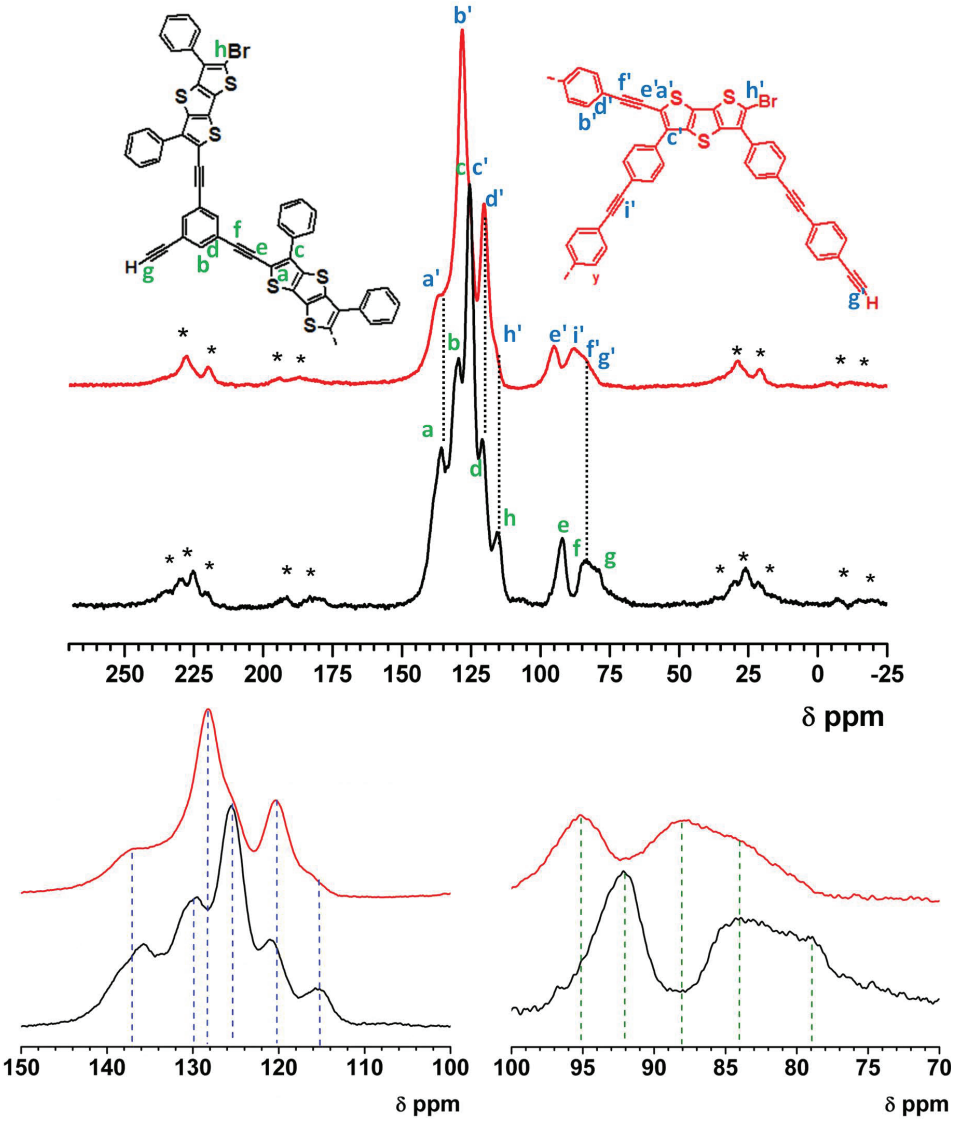

Figure 4. Solid state CP-MAS ^{13}C NMR spectra of DTT-CMP-DEB (red) and DTT-CMP-TEB (black). Asterisks are used to indicate spinning side bands.

For the acetylenic region (between 95 ppm and 78 ppm), the observed peaks provide more information related to the different backbones of the polymeric networks. For example, DTT-CMP-TEB is expected to display just one type of acetylenic connection since the dibromo-DTT derivative (monomer 2 in Figure 1) can only react with 1,3,5-ethynyls of TEB to form the final poly-aryleneethynylene. The two signals at 92.2 ppm

and 84.0 ppm can be assigned to that internal acetylene connection, which can be addressed to the carbon next to the α-position of DTT units and the carbon next to the benzene of TEB, respectively. In contrast, DTT-CMP-DEB was formed by A4 + B2 type monomers, among which the DTT moieties (A4, monomer 1 in Figure 1) act as crosslinkers and carry the reactive sites located in two different neighboring areas. Hence, three different acetylenic connections are expected in the spectrum of DTT-CMP-DEB (i.e. DTT≡DEB≡DTT, DTT≡DEB≡phenyl, phenyl≡DEB≡phenyl; see the drawing in Figure 1). Indeed, in the spectrum of DTT-CMP-DEB, an additional peak of the carbon-rich connection at 87.8 ppm (phenyl≡DEB≡phenyl) was spotted other than the ones that are nearly identical to the signals of DTT-CMP-TEB. Furthermore, the resonances of unreacted end groups were observed in both spectra at 115.6 ppm from the halogen-bearing α-carbon of DTT and at 78.5 ppm corresponding to terminal acetylenes.

IR measurements also revealed the structural variations for each CMP except the identical internal $C \equiv C$ stretching peak at 2183 cm^{-1} (Figure 5). Since DTT-CMP-DEB possessed only 1,4-difunctionalized benzene units, the three observed high intensity peaks in the IR spectrum at 1597 cm^{-1}, 1502 cm^{-1}, and 1404 cm^{-1} were attributed to $C = C$ stretching of benzene rings. On the other hand, in the same region, only two main peaks at 1577 cm^{-1} and 1443 cm^{-1} were observed for 1,3,5-trisubstituted benzenes of DTT-CMP-TEB along with multiple small peaks probably belonging to the monofunctionalized phenyl side group of the DTT linker.

Furthermore, $C - H$ out-of-plane bending of the benzene moieties along the polymeric networks also indicated altered responses in the spectra. In the studied frequency interval (900–690 cm^{-1}), 1,4-difunctionalized benzenes of DTT-CMP-DEB gave only one high intensity peak at 834 cm^{-1}. However, three strong peaks of DTT-CMP-TEB were observed at 875 cm^{-1}, 759 cm^{-1}, and 691 cm^{-1}, among which the first frequency should represent C-H of 1,3,5-trisubstituted benzenes, whereas the other two should be from monosubstituted phenyls connected to 3- and 5-positions of DTT units.

As was pointed in the introduction, changing the conjugation style affects the electronic properties of the final polymers. Therefore, the observed differences in the solid state diffuse reflectance UV/Vis (DRUV) measurements of the synthesized polymeric networks are not unexpected (Figure 6). Both DTT-CMP-TEB and DTT-CMP-DEB displayed broad absorptions in the visible region with maxima at 456 nm and 510 nm, respectively. A slight red shift of DTT-CMP-DEB could be due to its 1,4-connected benzene units, which enhance the conjugation length along the backbone, while such a conjugation is hindered by 1,3,5-substituted benzenes in DTT-CMP-TEB.

In conclusion, two similar CMPs, formed in different crosslinking patterns via Sonogashira–Hagihara polycondensation by respective coupling of di- and tetrabromo-DTT moieties (A2 and A4) with tri- and diethynyl-benzene units (B3 and B2), were presented. The effect of higher crosslinking with A4 + B2 type monomers resulted in higher microporosity. The polymer exhibited a larger accessible surface area with respect to the one with the B3 crosslinker. The polymers also exhibited altered spectral responses, which were explained via the change of the conjugation style and substituents along the backbone as a result of their different architectures. The presented results should be helpful when identifying complex POP structures such as the ones formed by using random copolymerization techniques (i.e. Friedel–Crafts alkylation to yield the traditional hypercrosslinked polymers or cross-coupling in the case of Yamamoto polymerization) or postsynthetic modifications (i.e. benzannulation over the triple bonds to form benzene moieties). Moreover, the effects of the conjugation length and pathway on the light absorption properties of CMPs were addressed, which are directly related to the electronic band gap of the materials, the tuning of which is essential for the

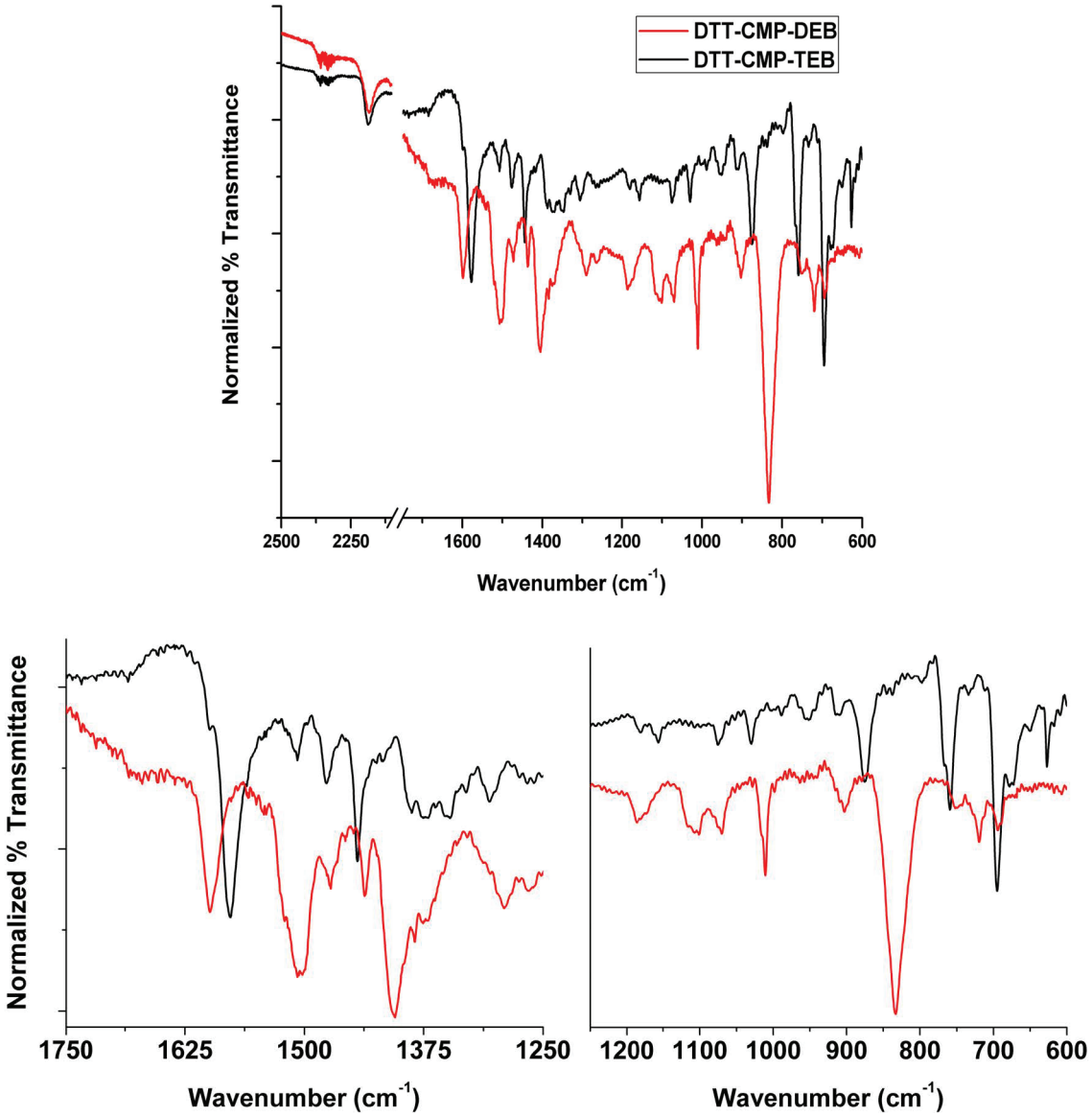

Figure 5. Infrared spectra (KBr) of DTT-CMP-DEB and DTT-CMP-TEB.

development of high performance CMPs to be used in electronic applications such as sensing, organic electronics, and photocatalysis.

3. Experimental

3.1. Materials and instrumentation

Monomer 1 and monomer 2 were synthesized according to the literature.[48] 1,3,5-triethynylbenzene (>98% GC, TEB) and 1,4-dietynylbenzene (>98% GC, DEB) were purchased from TCI Chemicals and further purified by a simple silica column, using dichloromethane (Carl Roth, 99.5%) as the eluent. $Pd(PPh_3)_4$ (99%), CuI (99.5%), dry diisopropylamine (99.95%, Sure/Seal), and dry triethylemine ($\geq$99.5%, Sure/Seal) were purchased from Sigma-Aldrich. Dry N,N-dimethylformamide (99.8%, Extra Dry, AcroSeal, DMF) was obtained from

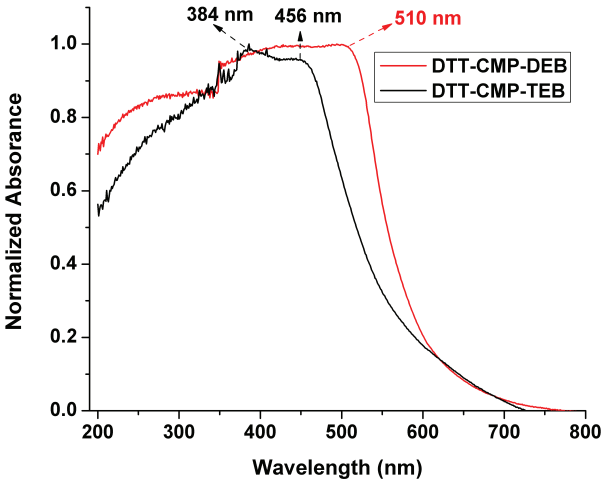

Figure 6. DR-UV/Vis spectra of DTT-CMP-DEB and DTT-CMP-TEB.

Acros Organics, which was used without any further purification. Solid state CP-MAS spectra were recorded on a Bruker Advance 400 MHz (100.6 MHz for ^{13}C measurements). Varian 640-IR and Varian Cary 300 spectrometers were used for infrared and diffuse reflectance UV-Vis spectroscopy measurements, respectively. N_2 gas sorption measurements were performed using an Autosorb iQ2. A Thermo FlashEA 1112 Organic Elemental Analyzer and Bruker D8 Advance were used for elemental analysis and p-XRD measurements, respectively.

3.2. Synthesis of DTT-CMP-DEB

In a glovebox, 250 mg (0.376 mmol) of 2,6-dibromo-3,5-bis(4-bromophenyl)bisthieno[3,2-*b*:2',3'-*d*]thiophene (monomer 1 in Figure 1), 94 mg (0.750 mmol) of DEB, 58 mg (0.050 mmol) of $Pd(PPh_3)_4$, and 9 mg (0.047 mmol) of CuI were dissolved in 25 mL of dry DMF and 2 mL of dry triethylamine in a 100 mL Schlenk flask, which was sealed afterwards and heated until 100 °C under inert atmosphere. After 3 days, the reaction mixture was cooled to room temperature, and the precipitation was filtered and washed with various solvents (100 mL THF, 50 mL MeOH, 50 mL distilled water, 50 mL $CHCl_3$, and again 50 mL MeOH). Further Soxhlet purification for the washed solid was performed in THF and MeOH for 1 day each, and it was finally dried under vacuum at 90 °C. Yield of the collected red powder (DTT-CMP-DEB) was 112% (yields above 100% are common for such materials, probably due to unreacted halogen endcaps). Elemental analysis for $C_{80}H_{32}S_6$: theoretical: %C 81.05, %H 2.72, %S 16.23 – found: %C 68.74, %H 2.71, %S 7.21 (the difference between theoretical and calculated values for elemental analysis is not unusual for such high dimensional amorphous polymeric structures, and it is probably due to the limited combustion in the polymeric core).

3.3. Synthesis of DTT-CMP-TEB

First 95 mg (0.187 mmol) of 2,6-dibromo-3,5-diphenylbisthieno[3,2-*b*:2',3'-*d*]thiophene (monomer 2 in Figure 1), 19 mg (0.126 mmol) of TEB, 14 mg (0.012 mmol) of $Pd(PPh_3)_4$, and 2 mg (0.01 mmol) of CuI were solved in 15 mL of dry DMF and 1 mL of dry diisopropyl amine under inert atmosphere (in glovebox), and then the charged 100 mL Schlenk flask was sealed and introduced to a 100 °C oil bath. The final precipitate was purified by following the same process mentioned above, yielding a pale yellow powder in 65% yield. Elemental analysis for $C_{84}H_{36}S_9$: theoretical: %C 75.65, %H 2.72, %S 21.63 – found: %C 66.79, %H 2.93, %S 13.00.

Acknowledgment

I would like to thank Prof Dr Turan Öztürk from İstanbul Technical University and Prof Dr Arne Thomas from the Technical University of Berlin for granting me access to use their chemicals and instruments.

References

1. Das, S.; Heasman, P.; Ben, T.; Qiu, S. *Chem. Rev.* **2017**, *117*, 1515-1563.
2. Dawson, R.; Cooper, A. I.; Adams, D. J. *Prog. Polym. Sci.* **2012**, *37*, 530-563.
3. Rose, M. *ChemCatChem* **2014**, *6*, 1166-1182.
4. van der Waal, J. C.; van Bekkum, H. *J. Porous Mater.* **1998**, *5*, 289-303.
5. Masters, A. F.; Maschmeyer, T. *Microporous Mesoporous Mater.* **2011**, *142*, 423-438.
6. Slater, A. G.; Cooper, A. I. *Science* **2015**, *348*, aaa8075.
7. Kumar, K. V.; Preuss, K.; Titirici, M. M.; Rodríguez-Reinoso, F. *Chem. Rev.* **2017**, *117*, 1796-1825.
8. Oschatz, M.; Antonietti, M. *Energy Environ. Sci.* **2018**, *11*, 57-70.
9. Wong, Y. L.; Tobin, J. M.; Xu, Z.; Vilela, F. *J. Mater. Chem. A* **2016**, *4*, 18677-18686.
10. Vyas, V. S.; Lau, V. W. H.; Lotsch, B. V. *Chem. Mater.* **2016**, *28*, 5191-5204.
11. Dalapati, S.; Gu, C.; Jiang, D. *Small* **2016**, *12*, 6513-6527.
12. Skabara, P. J.; Arlin, J. B.; Geerts, Y. H. *Adv. Mater.* **2013**, *25*, 1948-1954.
13. Bildirir, H.; Gregoriou, V. G.; Avgeropoulos, A.; Scherf, U.; Chochos, C. L. *Mater. Horizons* **2017**, *4*, 546-556.
14. Weber, J.; Thomas, A. In *Nanoporous Materials: Synthesis and Applications*; Xu, Q., Ed.; Taylor & Francis: Milton Park, UK, 2013, pp. 1-42.
15. Li, B.; Gong, R.; Wang, W.; Huang, X.; Zhang, W.; Li, H.; Hu, C.; Tan, B. *Macromolecules* **2011**, *44*, 2410-2414.
16. Dadashi-Silab, S.; Bildirir, H.; Dawson, R.; Thomas, A.; Yagci, Y. *Macromolecules* **2014**, *47*, 4607-4614.
17. Tsyurupa, M. P.; Davankov, V. A. *React. Funct. Polym.* **2006**, *66*, 768-779.
18. Tan, L.; Tan, B. *Chem. Soc. Rev.* **2017**, *46*, 3322-3356.
19. Abbott, L. J.; Colina, C. M. *Macromolecules* **2014**, *47*, 5409-5415.
20. Woodward, R. T.; Stevens, L. A.; Dawson, R.; Vijayaraghavan, M.; Hasell, T.; Silverwood, I. P.; Ewing, A. V.; Ratvijitvech, T.; Exley, J. D.; Chong, S. Y. et al. *J. Am. Chem. Soc.* **2014**, *136*, 9028-9035.
21. Chaoui, N.; Trunk, M.; Dawson, R.; Schmidt, J.; Thomas, A. *Chem. Soc. Rev.* **2017**, *46*, 3302-3321.
22. Feng, X.; Ding, X.; Jiang, D. *Chem. Soc. Rev.* **2012**, *41*, 6010-6022.
23. Huang, N.; Wang, P.; Jiang, D. *Nat. Rev. Mater.* **2016**, *1*, 16068.
24. Wu, J.; Xu, F.; Li, S.; Ma, P.; Zhang, X.; Liu, Q.; Fu, R.; Wu, D. *Adv. Mater.* **2018**, *0*, 1802922.
25. Schmidt, J.; Werner, M.; Thomas, A. *Macromolecules* **2009**, *42*, 4426-4429.
26. Ben, T.; Ren, H.; Shengqian, M.; Cao, D.; Lan, J.; Jing, X.; Wang, W.; Xu, J.; Deng, F.; Simmons, J. M. et al. *Angew. Chemie Int. Ed.* **2009**, *48*, 9457-9460.
27. Pei, C.; Ben, T.; Qiu, S. *Mater. Horizons* **2015**, *2*, 11-21.
28. Li, M.; Ren, H.; Sun, F.; Tian, Y.; Zhu, Y.; Li, J.; Mu, X.; Xu, J.; Deng, F.; Zhu, G. *Adv. Mater.* **2018**, *30*, 1804169.
29. Miyaura, N.; Suzuki, A. *Chem. Rev.* **1995**, *95*, 2457-2483.

30. Jiang, J. X.; Su, F.; Trewin, A.; Wood, C. D.; Campbell, N. L.; Niu, H.; Dickinson, C.; Ganin, A. Y.; Rosseinsky, M. J.; Khimyak, Y. Z. et al. *Angew. Chemie Int. Ed.* **2007**, *46*, 8574-8578.

31. Roeser, J.; Prill, D.; Bojdys, M. J.; Fayon, P.; Trewin, A.; Fitch, A. N.; Schmidt, M. U.; Thomas, A. *Nat. Chem.* **2017**, *9*, 977.

32. Yahiaoui, O.; Fitch, A. N.; Hoffmann, F.; Fröba, M.; Thomas, A.; Roeser, J. *J. Am. Chem. Soc.* **2018**, *140*, 5330-5333.

33. Jiang, J. X.; Su, F.; Trewin, A.; Wood, C. D.; Niu, H.; Jones, J. T. A.; Khimyak, Y. Z.; Cooper, A. I. *J. Am. Chem. Soc.* **2008**, *130*, 7710-7720.

34. Dawson, R.; Laybourn, A.; Khimyak, Y. Z.; Adams, D. J.; Cooper, A. I. *Macromolecules* **2010**, *43*, 8524-8530.

35. Bildirir, H.; Paraknowitsch, J. P.; Thomas, A. *Chem. A Eur. J.* **2014**, *20*, 9543-9548.

36. Laybourn, A.; Dawson, R.; Clowes, R.; Hasell, T.; Cooper, A. I.; Khimyak, Y. Z.; Adams, D. J. *Polym. Chem.* **2014**, *5*, 6325-6333.

37. Trunk, M.; Herrmann, A.; Bildirir, H.; Yassin, A.; Schmidt, J.; Thomas, A. *Chem. A Eur. J.* **2016**, *22*, 7179-7183.

38. Bao, L.; Sun, H.; Zhu, Z.; Liang, W.; Mu, P.; Zang, J.; Li, A. *Mater. Lett.* **2016**, *178*, 5-9.

39. Räupke, A.; Palma-Cando, A.; Shkura, E.; Teckhausen, P.; Polywka, A.; Görrn, P.; Scherf, U.; Riedl, T. *Sci. Rep.* **2016**, *6*, 29118.

40. Bildirir, H.; Osken, I.; Schmidt, J.; Ozturk, T.; Thomas, A. *ChemistrySelect* **2016**, *1*, 748-751.

41. Kessler, F. K.; Zheng, Y.; Schwarz, D.; Merschjann, C.; Schnick, W.; Wang, X.; Bojdys, M. J. *Nat. Rev. Mater.* **2017**, *2*, 17030.

42. Bonillo, B.; Sprick, R. S.; Cooper, A. I. *Chem. Mater.* **2016**, *28*, 3469-3480.

43. Sprick, R. S.; Bonillo, B.; Sachs, M.; Clowes, R.; Durrant, J. R.; Adams, D. J.; Cooper, A. I. *Chem. Commun.* **2016**, *52*, 10008-10011.

44. Schwarz, D.; Kochergin, Y. S.; Acharjya, A.; Ichangi, A.; Opanasenko, M. V.; Čejka, J.; Lappan, U.; Arki, P.; He, J.; Schmidt, J. et al. *Chem. A Eur. J.* **2017**, *23*, 13023-13027.

45. Kochergin, Y. S.; Schwarz, D.; Acharjya, A.; Ichangi, A.; Kulkarni, R.; Eliášová, P.; Vacek, J.; Schmidt, J.; Thomas, A.; Bojdys, M. J. *Angew. Chemie Int. Ed.* **2018**, *57*, 14188-14192.

46. Cinar, M. E.; Ozturk, T. *Chem. Rev.* **2015**, *115*, 3036-3140.

47. Bildirir, H.; Osken, I.; Ozturk, T.; Thomas, A. *Chem. A Eur. J.* **2015**, *21*, 9306-9311.

48. Osken, I.; Gundogan, A. S.; Tekin, E.; Eroglu, M. S.; Ozturk, T. *Macromolecules* **2013**, *46*, 9202-9210.